JSEE Vol. 22, No. 4, 2020 DOI: 10.48303/jsee.2021.247792

Research Paper

On the 2D Characteristics of Small-Scale Trapezoidal Sedimentary Basins

Reza Movahedasl[1] and Mohammad Reza Ghayamghamian[2*]

1. Ph.D. Student, Disaster Risk Management Research Center, International Institute of Earthquake Engineering and Seismology (IIEES), Tehran, Iran
2. Professor, Disaster Risk Management Research Center, International Institute of Earthquake Engineering and Seismology (IIEES), Tehran, Iran,
*Corresponding Author; email: mrgh@iiees.ac.ir

Received: 07/04/2021
Revised: 27/11/2021
Accepted: 06/12/2021

ABSTRACT

Recent researches clearly revealed that the 1D lateral model fail to reproduce actual site response characteristics in complex wave propagation field. In spite of many available researches on 2D or 3D effects of large-scale basins, different 2D or 3D behavior of small-scale sedimentary basins, are not well understood and explained. In the previous study, the authors studied the effects of small-scale basins and found it very important, depending on the shape of the lateral irregularities. Among different shapes of lateral irregularities, the small trapezoidal basin shows special site amplification characteristics, which need to be examined further. In this paper, different aspects of small-scale trapezoidal basins such as slope angle, basin length, infill soil properties and basin thickness are parametrically investigated to clarify those effects on strong ground motion characteristics. For this purpose and in the absence of recorded earthquake data on such lateral irregularities, extensive parametrical studies are carried out by using finite difference numerical analysis. Then, huge numbers of trapezoidal small basin models are constructed and are simultaneously subjected to the earthquake motions in both horizontal and vertical directions. The site response at the points along the basin are analyzed in the frequency domain using Fourier spectral ratio, and in the time domain using the ratio of 2D horizontal and vertical peak ground accelerations with respect to 1D ones are defined as the horizontal and vertical aggravation factors (AG_H and AG_V). The AG_H and AG_V factors show large sensitivity to infill soil properties and thickness as well as slope angle. The AG_H shows large variation in the middle of small trapezoidal basin in the range of 1.5 to 2. Meanwhile, the AG_V shows large variation around the two basin edges with the values of 1.5 to 2.5. Finally, the outcomes provide some recommendations in design, and emphasize on the importance of 2D analysis in site effect estimation of small-scale trapezoidal basin.

Keywords:
Small-scale trapezoidal basin; 2D site effects; Horizontal and vertical aggravation factors; Finite Difference Method (FDM)

1. Introduction

The damage distribution in many earthquakes obviously reveals that the characteristics of earthquake ground motion depend strongly on the site effects. "Site Effects" expression is commonly used in earthquake engineering and in fact indicates a set of different events arising from the propagation of seismic waves in near surface of geological formations or in geometrically irregular configurations itself such as basins and may exert a crucial impact on the severity of damage and its spatial distribution during earthquakes. Engineers have traditionally evaluated site effects using a 1D explanation of local soil profile with reasonable success and a good approximation for some cases.

The successful deconvolution analysis conducted by Takahashi and Hirano [1] using a 1D soil model, which is reproduced in Aki and Larner [2] was probably the first quantitative evidence of this sort. Later, Kanai et al. [3] showed the agreement between observed spectral ratios of surface records relative to borehole ones and theoretical prediction using 1D soil models. However, developments and advances in array instrumental measurements show a remarkable complexity in site amplification characteristics. Results obtained from earthquake data analyses of downhole arrays show strong dependence of amplification pattern to the various features of near surface geology such as 2D or 3D shapes of lateral irregularities, which cannot be explained by conventional 1D model [4-9].

2D or 3D effects of large-scale basins or valleys (scales in several kilometers) have been known to influence strong ground motion characteristics in the low frequency range (<1 Hz) [10-15]. Complex effects of wave propagation in the surface layers, which actually include anisotropy, heterogeneity, irregular boundaries, etc., are manifested in different types of wave conversions and/or ground motion cross-coupling [5-6, 8]. Ghayamghamian [8] firstly introduced shear-wave coupling phenomena due to lateral irregularities in small-scale basins. He analyzed the local site effects using recorded earthquake ground motions at downhole array network in Sendai city, Japan. He noticed that the 2D shape of Sendai small basin could dramatically change the amplification characteristics of the site, especially in the vicinity of basin edge. Furthermore, a hypothesis to explain this phenomenon based on cross-coupling between two shear waves propagating in two sides of basin edge was introduced and an analytical model for coupled shear waves was developed. This coupled model successfully used to reproduce the observed amplification along the Sendai small basin [8]. These outcomes provide concrete field and theoretical evidence on the importance of small basin 2D effects. Furthermore, they gave more confirmation to the fact that in complex wave fields the motions in two or three orthogonal directions are dependent and cannot be separately treated due to the ground motion conversions and cross-coupling effects. It should be emphasized that in contrary to the large basins that extensively affect low frequency range (< 1 Hz) of ground motion, the small basins largely affect high frequency range (> 1 Hz).

In addition, the current seismic building codes are usually based on 1D model of soil profile in site effect estimation, and generally do not take into account 2D or 3D effects of subsurface irregularities. These made a motivation and necessity for further detailed investigations on different aspects of lateral irregularities to find their importance in design. In the absence of enough available earthquake data on different lateral irregularities and the limited data with clear understanding of subsurface geology, the parametric study was the only method for such purpose. Later on, Movahedasl and Ghayamghamian [9] conducted a parametric study on different aspects of lateral irregularities of small-scale basins to provide some recommendations to engineering practice. Among those parametric studies, the small trapezoidal basin showed special features, which need to be further investigated. Therefore, in this paper, we focused our investigation to the small trapezoidal basin and its different aspects such as slope angle, basin length, infill soil properties and basin thickness to give some insights in engineering practice and design code.

2. Methodology

To investigate 2D effects of a small trapezoidal basin, it is possible to consider modal approaches or directly investigate wave propagation phenomena in the time domain. Here, we employed numerical analysis in the time domain based on the Finite Difference Method (FDM) using FLAC computer program (Itasca 2012) [16], which allows a complete description of the amplification process. The calculation is based on the explicit finite difference scheme to solve the full equations of motion using lumped grid point masses derived from the real density of surrounding zones. Materials are assumed to be dry and linear elastic.

The parametric studies are carried out on the main features of small trapezoidal basin such as slope angle, basin length, infill soil properties and basin thickness. To this end, various small trapezoidal basin models are constructed and are simultaneously subjected to the horizontal and vertical earthquake motions to make the results

more realistic. Then, the output motions are calculated using FLAC computer program at different assumed points along the surface of the basin models. The 2D effects of small trapezoidal basin are examined both in the frequency and time domains. In the frequency domain, the 2D site response is estimated using Fourier spectral ratio of calculated surface motion to that of input motion at each point along the basin. In the time domain, the horizontal and vertical aggravation factors (AG_H and AG_V) are defined as the ratio of 2D horizontal and vertical surface peak ground accelerations (PGAs) to those of 1D ones, respectively. Then the variations of these factors at the points along the small trapezoidal basins are examined.

3. Modeling in FLAC and Dynamic Analysis Considerations

The calculation in FLAC is based on the explicit finite difference scheme. There are two sets of governing equations: the dynamic equilibrium and the constitutive equations. The first set of equations of dynamic equilibrium is the generalized Newton's law of motion for a continuous body, which is expressed as:

$$p\frac{\partial \dot{u}_i}{\partial t} = \frac{\partial \sigma_{ij}}{\partial x_j} + pg_i \tag{1}$$

where t is the time, $x(j)$ is the coordinate vector, ρ is the mass density, g_i is the gravitational acceleration, $\dot{u}_i$ is the velocity vector, and σ_{ij} is the stress tensor. The other set of equations is the constitutive relation, or stress-strain law, which has the following generic form:

$$\dot{\sigma}_{ij} = M(\sigma_{ij}, \dot{\varepsilon}_{ij}, q_n) \tag{2}$$

where $M(\,)$ is the functional form of the constitutive law, $\dot{\varepsilon}_{ij}$ represents strain rates and q_n are history parameters depending on the particular law. The strain rate $\dot{\varepsilon}_{ij}$ is derived from velocities gradients as follows:

$$\dot{\varepsilon}_{ij} = \frac{1}{2}\left[\frac{\partial \dot{u}_i}{\partial x_j} + \frac{\partial \dot{u}_j}{\partial x_i}\right] \tag{3}$$

The stability of the analysis is assured by the critical time step, which is automatically calculated by the FLAC program. The critical time step is calculated as follows:

$$\Delta t_{critical} = 2\sqrt{\frac{m_z A_z}{4\left(k + \frac{4}{3}G\right)L_d^2 T}} \tag{4}$$

where m_z is the mass of each rectangular zone, A_z is the area of the rectangular zone, and L_d the length of its diagonal, k the bulk modulus, G the shear modulus and T is the out-of-plane dimension, equal to 1.0 for a plane-strain analysis. However, the more general form is used in FLAC deriving the dynamic time step, Δt_d using a safety factor of 0.5 (to allow for the fact that the calculation of time step is an estimate only) as: $\Delta t_d = 0.5 * \Delta t_{critical}$ to achieve computing stability.

Both the frequency content of the input motion and the wave speed characteristics of the model will affect the numerical accuracy of wave transmission. Lysmer and Kuhlemeyer [17] showed that for accurate representation of wave transmission through a model, the spatial element size (l) must be smaller than approximately one-tenth to one-eighth of the wave length, associated with the highest frequency component of the input motion. In regard to the lowest shear wave velocity of the assumed infill soils in the trapezoidal basin models to be 200 m/s, and the highest frequency of 8Hz need to be captured, the element size is defined to be 2.5 m × 2.5 m in constructing of the small trapezoidal basin models. Furthermore, the input motions need to be also band pass filtered between 0.1 and 8 Hz, and the PGA of both components are scaled to assure the linear behavior of soil material. Appropriate artificial numerical boundaries are also used to allow the necessary energy radiation and to stop the outward propagation waves back into the model.

The viscous boundary developed by Lysmer and Kuhlemeyer [17] is used as Quiet/free field (absorbing) boundaries which are based on the use of independent dashpots in the normal and shear directions. Rayleigh damping is used to small strain damping. These two frequency schemes proposed for the first time by Rayleigh and Lindsay [18]. The use of a two-frequency scheme allows the model to respond to the predominant frequencies of the input motion without experiencing significant over-dam-ping. Kwok et al. [19] recommended a

value equal to five times of the natural frequency. This recommendation is used to successfully model small strain damping. The procedure for accurate estimation of damping in the models, wave transmission and boundary conditions were explained in detail in Movahedasl and Ghayamghamian [9] and would not be repeated here due to the space limitation.

4. Fujisawa Small Basin

The Fujisawa small-scale basin, crossed by a bridge (Ohba Ohashi Bridge which is a 600 m long road bridge built across Hikichi River), consists of shallow sediments of very soft soil confined by a relatively-stiff base and steep lateral subterraneous slopes near Fujisawa City, Kanagawa prefecture, Japan (Figure 1). Detailed geophysical and geotechnical investigations were carried out at the site and the soil properties of the layers were defined as depicted in Figure (2). Site geologic profile consists of approximately 22 m of soft alluvium (extremely soft clayey strata, containing humus and silt) with the shear-wave velocity (measured by downhole tests) ranging from 40 to 65 m/s. The underlying sub-stratum consists of layers of stiff clay and sand characterized by N values over 50 and shear-wave velocity of about 400 m/s [20-24].

At Fujisawa site, a downhole array was also established by the Institute of Technology of Shimizu Corporation. The objective was to evaluate site effects and to develop a rational seismic design method. The downhole was equipped with feed-back-type accelerometers with a sampling rate of 50 samples per second. Two accelerometers were arranged vertically at surface (-1 m) and at a depth of -30 m as shown by Points A and B in Figure (1b). The downhole arrays are favorable in site effect estimation due to the effective removal of source and path effects by the spectra ratio of surface record to that of one at depth.

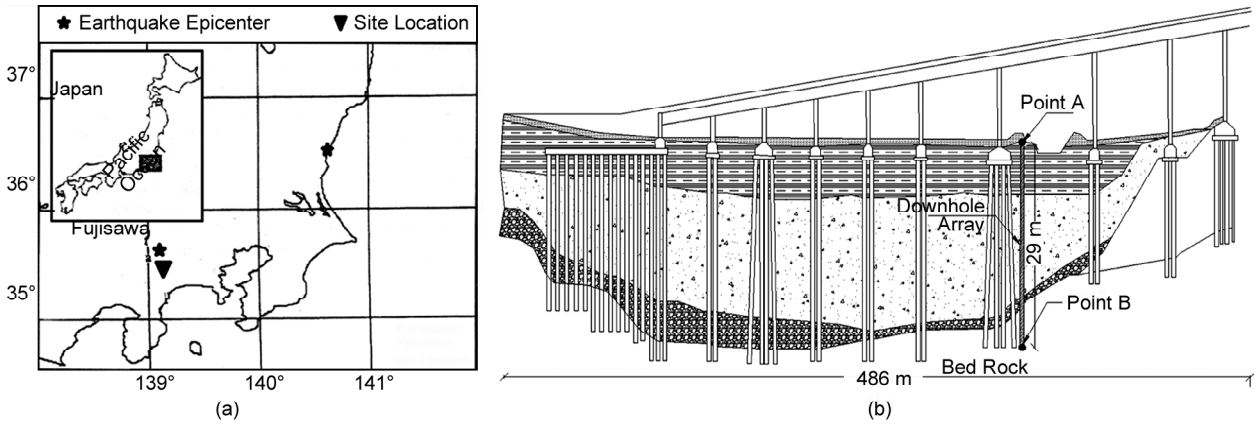

Figure 1. The soil profile characteristics at Fujisawa downhole array site.

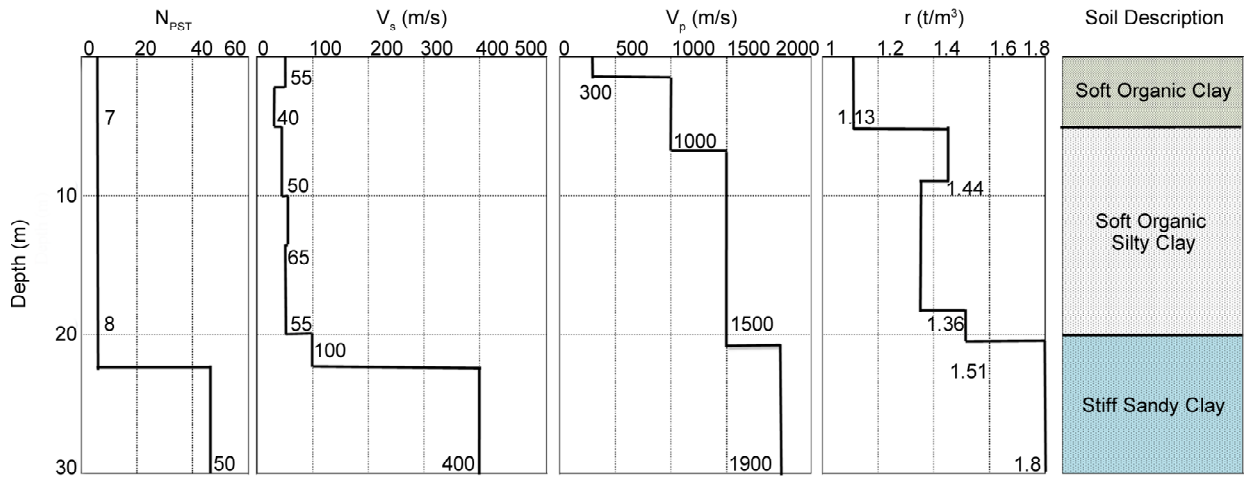

Figure 2. The soil profile characteristics at Fujisawa downhole array site.

Two earthquake data with different epicentral distances are selected from Strong Motion Array Recorded Database in Japan published by the Association for Earthquake Disaster Prevention [25]. The parameters of selected earthquakes (hereafter referred to as Earthquake 1 and Earthquake 2) are listed in Table (1). Note that the peak ground acceleration of the selected records is small enough to preserve soil linear behavior at the site. These recordings are used to evaluate horizontal and vertical amplification functions using Fourier spectral ratio of surface accelerometers to those of depth ones.

In the next step, the 2D model of Fujisawa small basin is constructed and is numerically analyzed using FLAC computer program to find a possible explanation to the observed spectral ratios at downhole array site in Fujisawa small basin. Figure (3) shows the simplified 2D model of Fujisawa small basin and its geotechnical parameters, which is inferred from conducted geophysical and geotechnical investigations at the site. The biggest grid size is defined to be 0.8 m × 0.8 m in regard with the lowest shear wave velocity of the infill soil (V_s = 60 m/s) and the highest frequency of 5 Hz need to be captured. The model is simultaneously excited by recorded horizontal and vertical earthquake motions at depth (point B) for both earthquakes 1 and 2. Then, the horizontal and vertical acceleration time histories at surface (point A) are calculated by FLAC program assuming the linear behavior of the overlying soil. Figure (4) compares the observed and calculated horizontal and vertical motions at surface, which show good agreements.

Note that the observed surface horizontal and vertical motions in this figure are band pass filtered in the range of 0.15 to 5 Hz due to the element size of the model, which controls the acceptable frequency range in the 2D numerical analysis. Furthermore, the 2D horizontal and vertical amplification functions are calculated using Fourier spectral ratio of surface motions to those of depth motions. In Figure (5), the calculated 2D amplification functions are compared with 1D and observed ones. The observed vertical spectral ratios show totally different characteristics with those of theoretical 1D ones for both earthquakes.

It is noteworthy that the theoretical 1D vertical amplification function is flat up to 12 Hz and show a first peak frequency at 15 Hz. For horizontal component, it is evident that the 1D theoretical amplification functions failed to explain some peak frequencies and their values in the observed spectral ratios from earthquake data. The 2D amplification functions for both horizontal and vertical motions show good agreements with the observed ones. This provides a good confirmation to the 2D site effects of Fujisawa small basin and its importance at the sites with lateral irregularities. Furthermore, AG_H and AG_V is calculated along the Fujisawa basin and shown in Figure (6), respectively.

Table 1. The parameters of the selected earthquakes.

Earthquake No.	Date yr.m.d.	Depth (Km)	M (JMA)	Epicentral Distance (km)	Point A		Point B	
					HPGA (m/s^2)	VPGA (m/s^2)	HPBA (m/s^2)	VPBA (m/s^2)
1	1982.03.07	60	5.5	163.9	0.075	0.0298	0.015	0.011
2	1984.02.04	25	5.2	25	0.255	0.129	0.0893	0.034

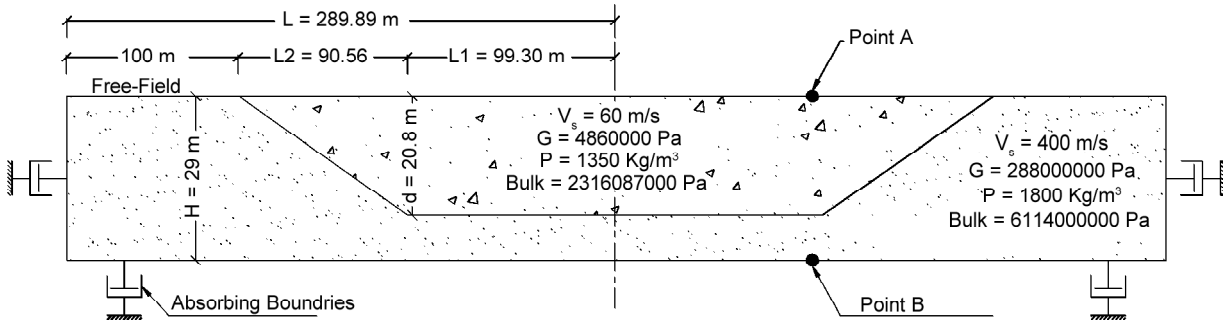

Figure 3. Simple geometry of the model, absorbing boundaries and assumed soil properties inferred from conducted geophysical and geotechnical investigations. Points A and B show the locations of uphole and depth accelerometers at Fujisawa downhole array.

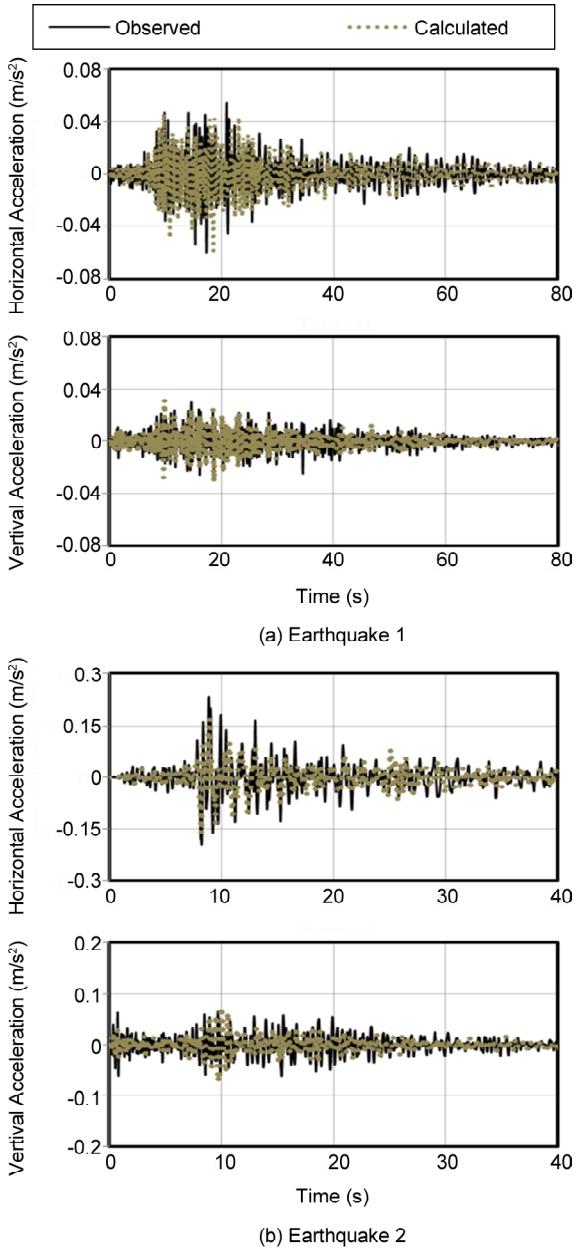

Figure 4. Comparison between recorded (band pass filtered in the range of 0.15 to 5 Hz) and computed ground motions in horizontal and vertical directions.

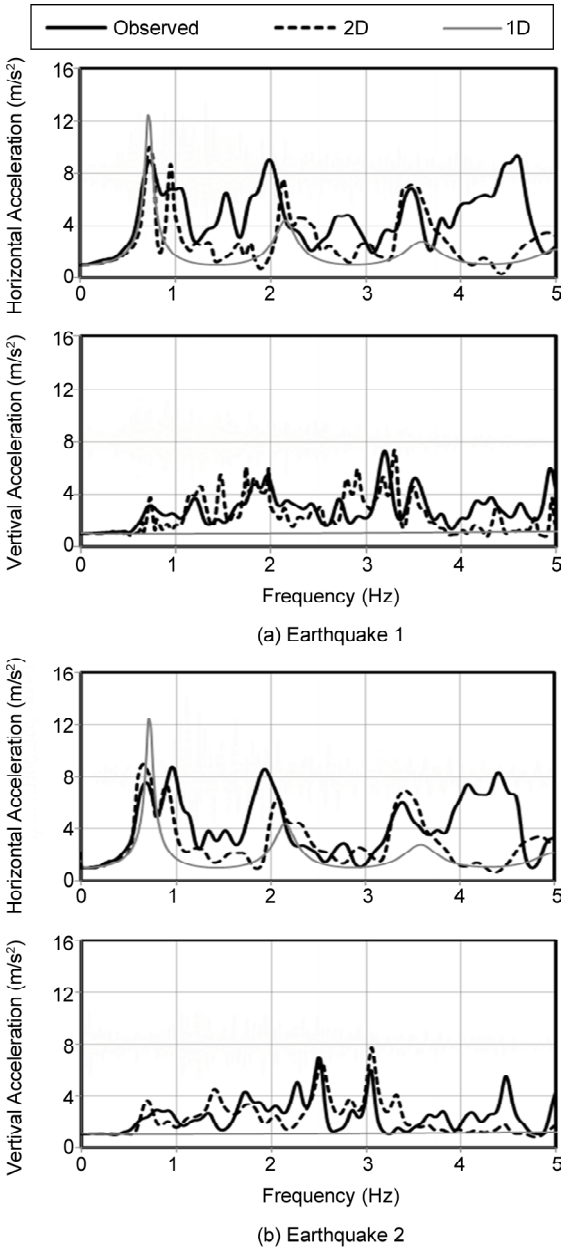

Figure 5. Comparison among observed horizontal and vertical spectral ratios with those of 1D and 2D calculated models.

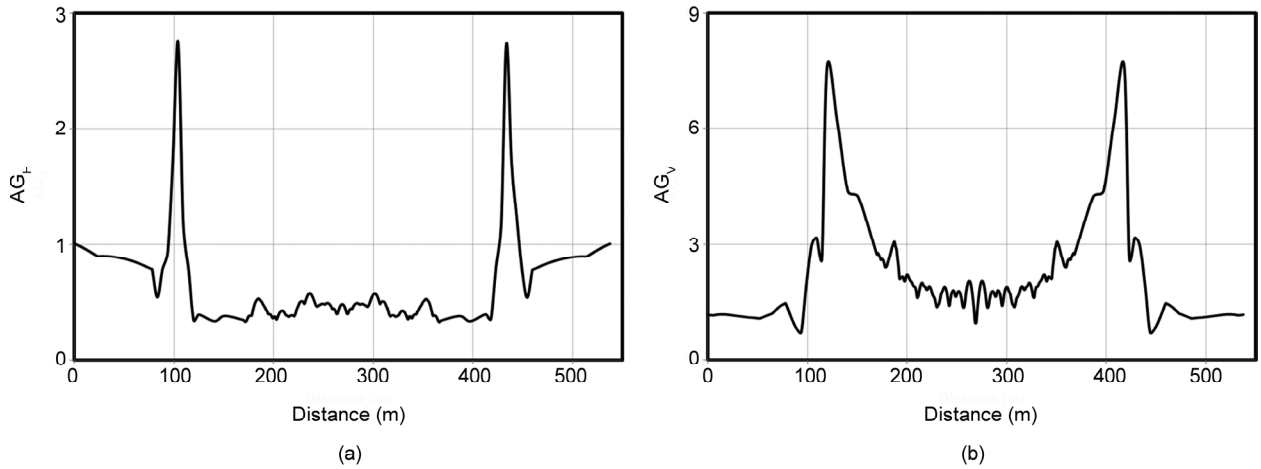

Figure 6. The variations of (a) horizontal and (b) vertical aggravation factors along the Fujisawa basin.

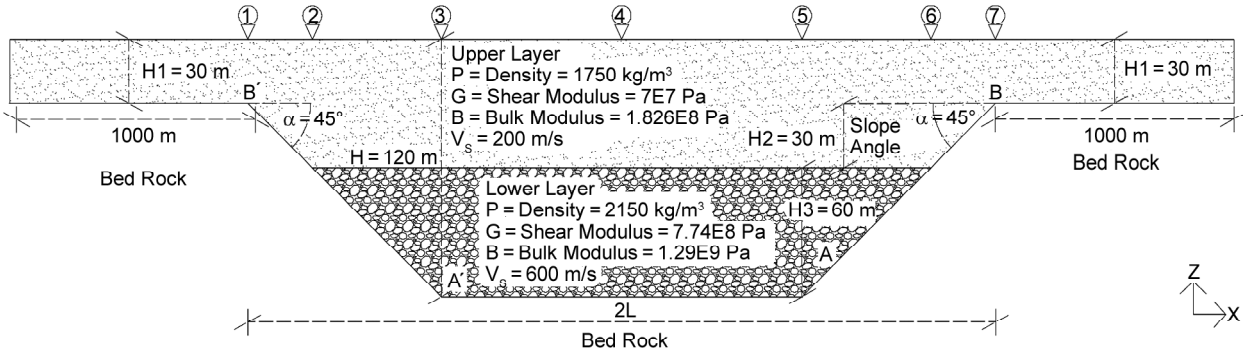

Figure 7. The assumed small trapezoidal basin model and its parameters.

5. 2D Analysis of a Small Trapezoidal Basin and Assumptions of Input Motions

In this chapter, we first assumed a typical small trapezoidal basin and examined its behavior under two assumptions for input motion. First, the horizontal or vertical motion is separately applied. Second, the horizontal and vertical motions are simultaneously applied. Figure (7) shows the assumed trapezoidal basin and its specifications. The numbers along the basin surface show the locations of the assumed points, where the surface motions and then 2D basin amplification characteristics will be calculated. The surface horizontal and vertical acceleration time histories numerically calculated by using FLAC computer program, which is very well-known and widely used software for numerically modeling geotechnical earthquake engineering problems.

These time histories are analyzed in the frequency and time domains to show how the small trapezoidal basin affects site amplification and dominant frequency characteristics as well as PGAs due to its lateral irregularities as will be explained in the following.

5.1. Frequency Domain Analysis

In the frequency domain analysis, the 2D horizontal and vertical amplification functions are computed using Fourier spectral ratio of calculated surface motion to that of input motion at the points along the basin for each assumed case. Furthermore, the 1D soil amplification functions for the soil profiles at the points are also calculated. The obtained horizontal and vertical spectral ratios (HSRs and VSRs) at these points are depicted in Figures (8) and (9), respectively. In these figures, the 2D-1comp and 2D-2comp represent the assumed two cases of input motion in 2D analysis.

In Figure (8), the 2D horizontal amplification functions reveal clear difference in both frequencies and amplification values compared to the theoretical 1D prediction. All the points almost show two or three peak frequencies with low amplification values around the 1D peak frequencies, as shown by the grey arrows. The reason of such phenomena was already explained by Ghayamghamian [8] based on shear wave coupling hypothesis. Furthermore, comparing the 2D-1comp and 2D-2comp amplification functions, a clear peak is appeared around 3 Hz at points 1, 2, 6 and 7 for the 2D-2comp case as shown by black arrows in Figure (8). As getting distance from the basin edges (points 3 to 5), the 2D-2comp and 2D-1comp responses are getting similar, while there are still very significant difference between the 1D and 2D HSRs at these points. The comparison between 1D and 2D spectral ratios of small trapezoidal basin demonstrate that the actual site response inside the small trapezoidal basin cannot be explained by the 1D method due to the lateral irregularities.

The 2D vertical spectral ratios (VSRs) at the points along the basin are also compared with the 1D vertical ones [26-27] in Figure (9). In contrast to 2D horizontal spectral ratios, the vertical spectral ratios show a clear difference at the points 1, 2, 6 and 7 around the basin edges. However, except for some small differences, the 2D vertical spectral ratios are more or less the same at the points 3, 4 and 5 toward the inside of trapezoidal basin. Furthermore, the comparison of 2D-1comp and 2D-2comp shows two other peak frequencies around 1 and 4.5 Hz as shown by black arrows.

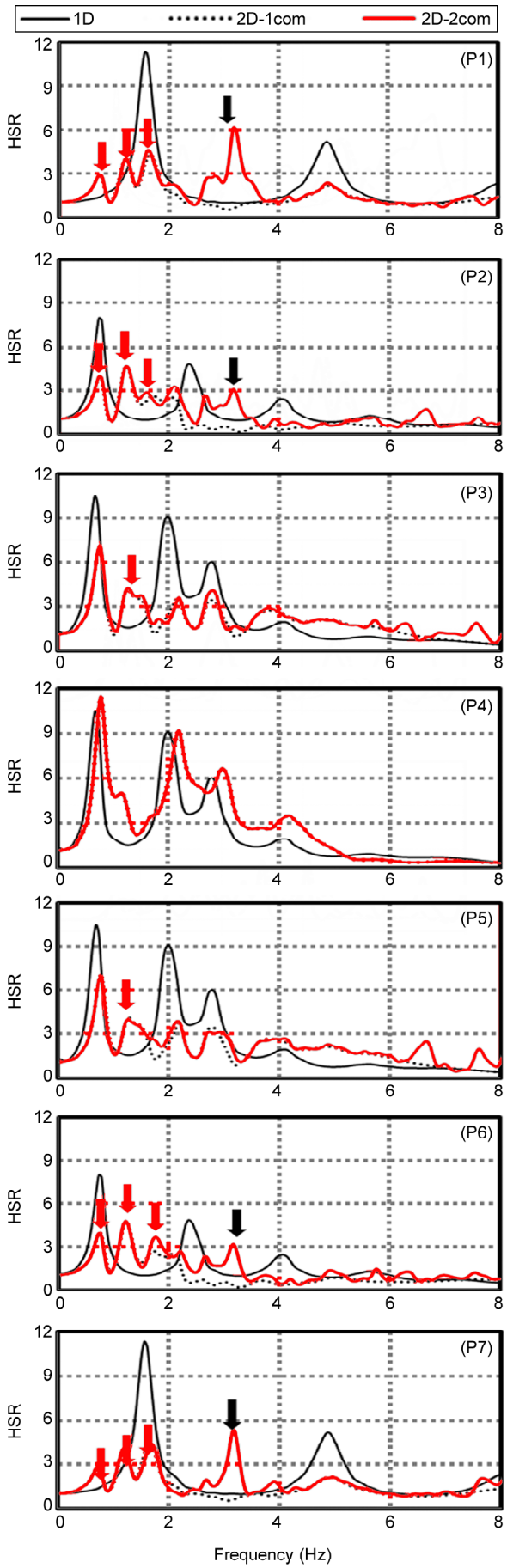

Figure 8. Horizontal spectral ratios (HSRs) at the assumed points along the trapezoidal small basin surface compared with 1D theoretical amplification functions.

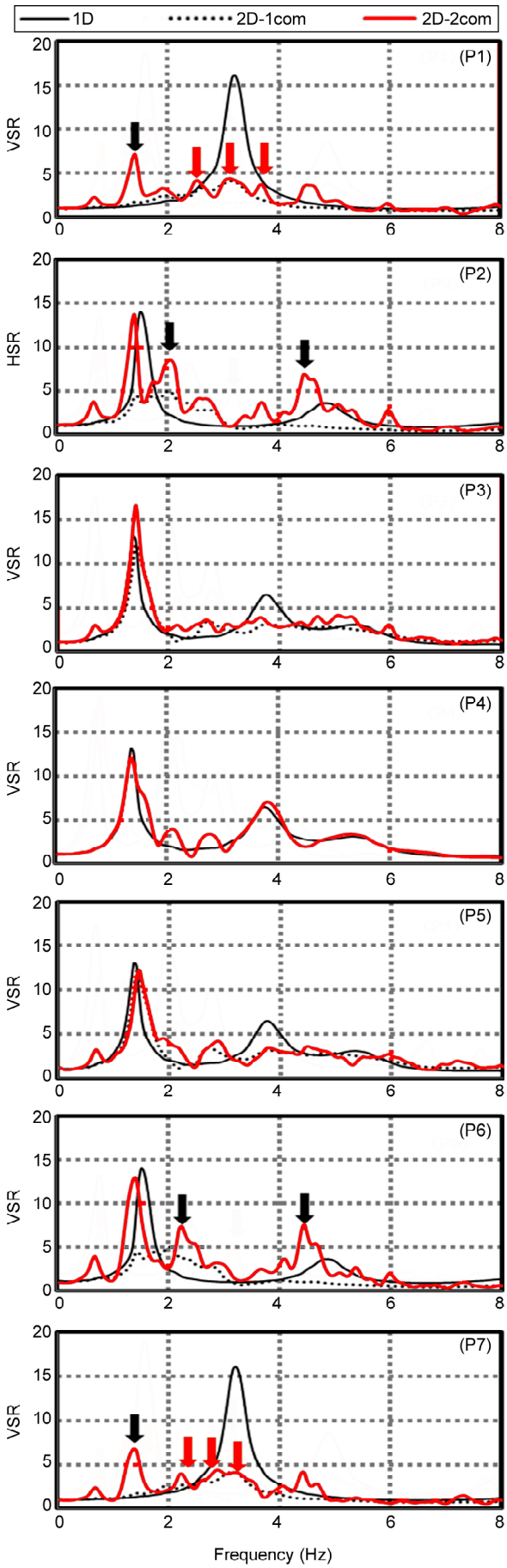

Figure 9. Vertical spectral ratios (VSRs) at the assumed points along the trapezoidal small basin surface compared with 1D theoretical amplification functions.

The results also show that not only the wave coupling occurs at the edges in two sides of trapezoidal basin, but also the interferences introduce new peak frequencies with different peak values, the appearance of which in the spectral ratios depend on the distance measuring point location with respect to basin edges. It is also shown that applying a single excitation in only one direction may mislead the results, and the motions in different orthogonal directions need to be accounted for getting more realistic results.

5.2. Time Domain Analysis

The observed differences in computed spectral ratios make a motivation to examine how these differences affect the characteristics of ground motion in the time domain. Here, we define two new factors as:

$$AG_H = \frac{PGA_H^{(2D)}}{PGA_H^{(1D)}} \tag{5}$$

and

$$AG_V = \frac{PGA_V^{(2D)}}{PGA_V^{(1D)}} \tag{6}$$

where $PGA^{(2D)}$ and $PGA^{(1D)}$ are 2D and 1D peak ground accelerations at surface, respectively. *H* and *V* subscripts stand for the horizontal and vertical components.

Using calculated surface motions for 2D and 1D analysis, the AG_H and AG_V are computed and their variations along basin are examined for separate excitation of horizontal or vertical motion as shown in Figure (10a). In this figure, the AG_H and AG_V factors are calculated for each 2.5 m instead of defined points (points 1 to 7 in Figure 7), in order to get the smooth variations of these factors with distance. Furthermore, the horizontal distance along the basin is normalized to the basin half-length (L in Figure 7). As expected from the calculated horizontal spectral ratios in Figure (8), the AG_H decrease from points 1 to 3 and 5 to 7 near the basin edges and gradually increase to 1.5 with getting distant from the edges. The PGA_H^{2D} increases almost 53% in the middle of the basin (point 4) and decreases almost 47% around the edges (points 1, 2, 6 and 7) compared to the PGA_H^{2D} due to the lateral irregularity in small trapezoidal basin.

Figure (10b) shows the variations of the AG_H and AG_V for the simultaneous excitations in horizontal and vertical directions. As it is shown in Figure (10b), the general trend is the same except for the maximum and minimum values that are a little smaller than those shown in Figure (10a). This may be attributed to the conversion of the horizontal motion to the vertical one at these points. The reverse trend can be seen caused by the vertical motion conversion to the horizontal one.

The results of the frequency and time domain analyses provide important outcomes that can play a significant role in design of critical facilities, bridges and lifelines. They show that the AG_H and AG_V largely fluctuate in the middle and around the basin edges, which could be increasing or decreasing, depend on the distance to the small trapezoidal basin edges. They also strongly emphasize that the conventional 1D model would generally fail to reproduce the complex wave propagation and scattering effects introduced by the lateral irregularity of small trapezoidal basin.

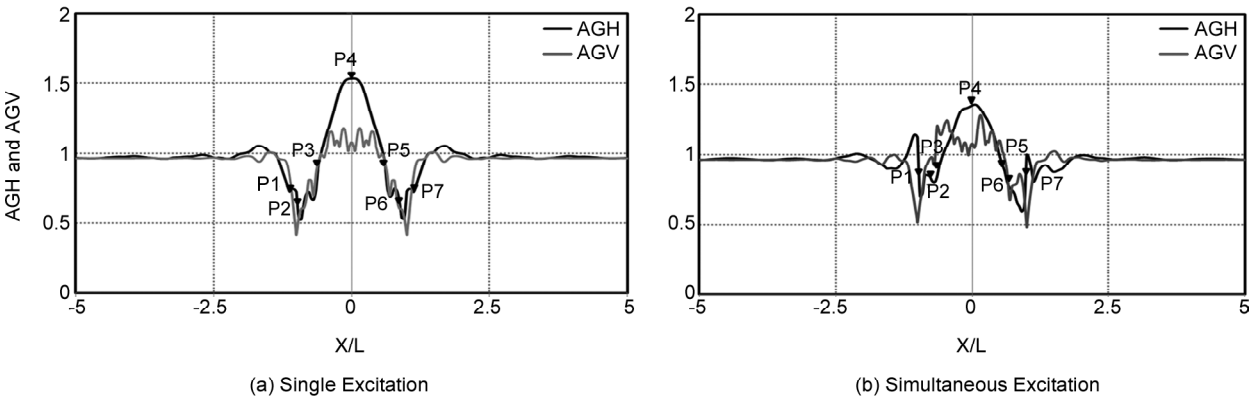

Figure 10. The variations of aggravation factors along the small basin model.

6. Parametric Study on the Small Trapezoidal Basin

The importance of 2D and/or 3D effects of small trapezoidal basin has not been well understood yet in engineering practice. In order to clarify different aspects of small trapezoidal basin on ground motion characteristics, and in the absence of recorded earthquake data, an extensive parametric study on the main features of the small trapezoidal basin needs to be carried out. The main features such as basin slope angle, length, thickness and infill soil properties need to be parametrically investigated. For this purpose, numerous 2D models of small trapezoidal basin are constructed, and are subjected to the earthquake ground motions.

Due to the wave field complexity and considering the results in section 5, horizontal and vertical input motions are simultaneously applied to the models. Basin model and its general specifications are the same as those shown in Figure (7). The model is defined with two layers and an underlying bedrock. The soil behavior is assumed to be dry and linear elastic. The specifications of soil layers are listed in Table (2). In parametric study, the surface motions are calculated at each 2.5 m distance along the basin. Therefore, due to the large number of models and calculated surface motions, the results are only presented using the variation horizontal and vertical aggravation factors along the basin.

6.1. Basin Slope Angle

The trapezoidal basin models with various slopes of 30, 45, 60 and 90 degrees are constructed to examine the slope angle variation effects. Meanwhile, the other parameters shown in Figure (1) are assumed to be constant. The variations of the AGH and AGV factors are calculated for each case as shown in Figure (11). From this figure, it can be seen that, the AG_H and AG_V factors increase with increasing of slope angle in the center of the basin. The maximum PGA_H^{2D} is almost 1.75 times larger and its minimum is 0.45 times smaller than those of PGA_H^{2D} in a distance range of $-2 < X / L < 2$. However, the maximum PGA_V^{2D} is almost 1.5 times larger and 0.5 smaller than those of PGA_V^{1D} in a distance range of $-1.25 < X / L < 1.25$.

6.1. Small Basin Length

To study the basin length effects, a new term is

Table 2. Geotechnical specifications of infill soil materials of small basin.

Soil Properties / Soil Layers	Mass Density (kg/m^3)	Maximum Shear Modulus (Pa)	Bulk Modulus (Pa)	Shear Wave Velocity (m/s)	Poisson Ratio
Upper Layer	1750	0.7E8	0.18E9	200	0.33
Lower Layer	2150	7.74E8	1.29E9	600	0.25
Bed Rock	2600	37.44E8	4.992E9	1200	0.20

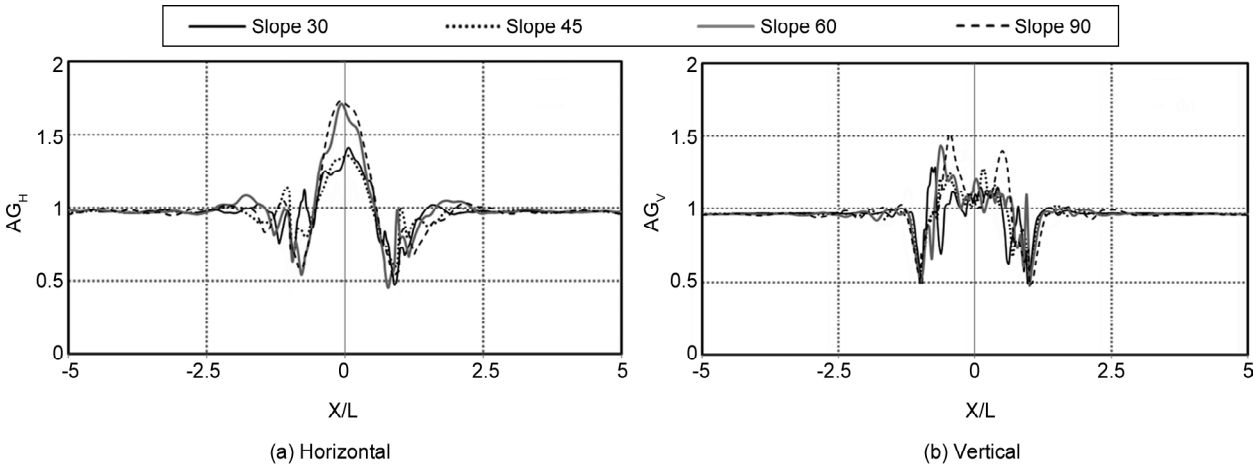

Figure 11. The variations of (a) horizontal and (b) vertical aggravation factors along the small trapezoidal basin models for slope angles of 30, 45, 60 and 90.

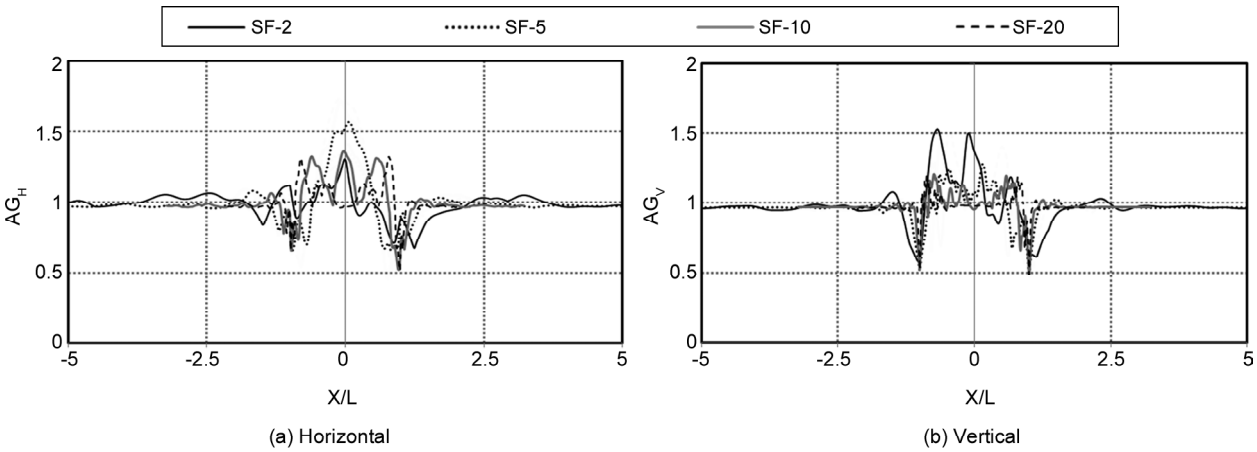

Figure 12. The variations of (a) horizontal and (b) vertical aggravation factors along the trapezoidal small basin models for shape factors of 2, 5, 10 and 20.

defined as the ratio of L to H (Figure 7) and called as shape factor (SF). In construction of small trapezoidal basin models with different length, the H parameter is assumed to be constant and the variation is made on L length. The slope angle is also fixed to be 45 degree at the both edges. Soil properties are assumed to be the same as those given in Table (2). The models with different shape factors of 2, 5, 10 and 20 are constructed, and are analyzed in the same fashion already described. Figure (12) shows the variations of the AG_H and AG_V factors along the trapezoidal basin for different shape factors.

From Figure (12), the AG_H factor show a clear single peak for $SF<5$ in the middle of trapezoidal basin $(X/L=0)$ with a maximum value of 1.55. Meanwhile, the AG_V factor show two peaks with the maximum value of 1.5 at $X/L<0$. In $SF=10$, a single peak of AG_H becomes three distinct peaks with the same values of 1.3 at $-1<X/L<1$, while the AG_V factor show a small peaks at $-1<X/L<1$. For the largest one (i.e. $SF=20$), the AG_H shows two distinct peaks with a value of 1.2 at $-1.2<X/L<1.2$. It is interesting to see that both AG_H and AG_V factors show two minimums with the values in the range of 0.25 to 0.5 at $-1.25<X/L$ and $X/L>1.25$.

6.3. Soil Properties

To estimate the effects of infill soil properties on small trapezoidal basin response, trapezoidal basin models with different wave velocities of soil layers are made. For simplicity, the soil properties of only upper layer are varied and four cases are assumed as summarized in Table (3). All other parameters left to be the same as those shown in Figure (1). The variations of AG_H and AG_V factors along the basin for different cases (M1-M4 in Table 2) are calculated in the same fashion and shown in Figure (13).

From this figure, the number of AGH peak increases with decreasing impedance ratio. The AG_H peak values decrease with decreasing impedance ratio. Meanwhile, the AGV values and number of peaks show a reverse trend compared with AG_H. The AG_V value increases with decreasing impedance ratio.

6.4. Small Basin Thickness

Figure (14) shows a schematic model with two thickness parameters ($H1$ and $H2$) at two sides of the small basin edge. The soil properties are

Table 3. Various geotechnical specifications assumed for upper layer.

Case No.	Mass Density (kg/m^3)	Maximum Shear Modulus (Pa)	Bulk Modulus (Pa)	Shear Wave Velocity (m/s)	Poisson Ratio	Impedance Ratio
M1	1750	0.7E8	1.8285E8	200	0.33	3.7
M2	1850	1.665E8	3.8266E8	300	0.31	2.3
M3	1950	3.12E8	6.3886E8	400	0.29	1.6
M4	2050	5.125E8	9.4330E8	500	0.27	1.3

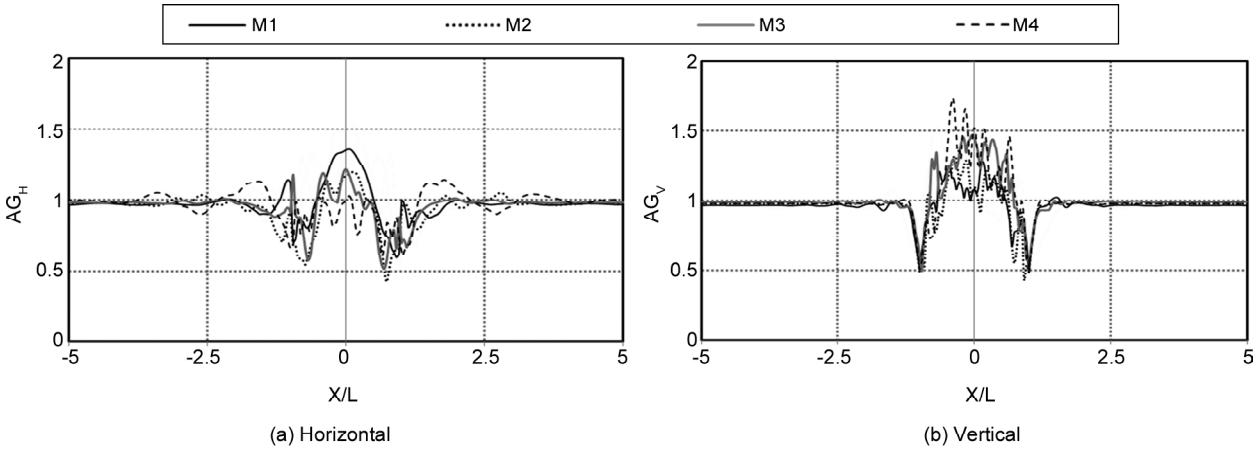

Figure 13. The variations of (a) horizontal and (b) vertical aggravation factors along the trapezoidal small basin models for impedance ratio of 3.7, 2.3, 1.6 and 1.3.

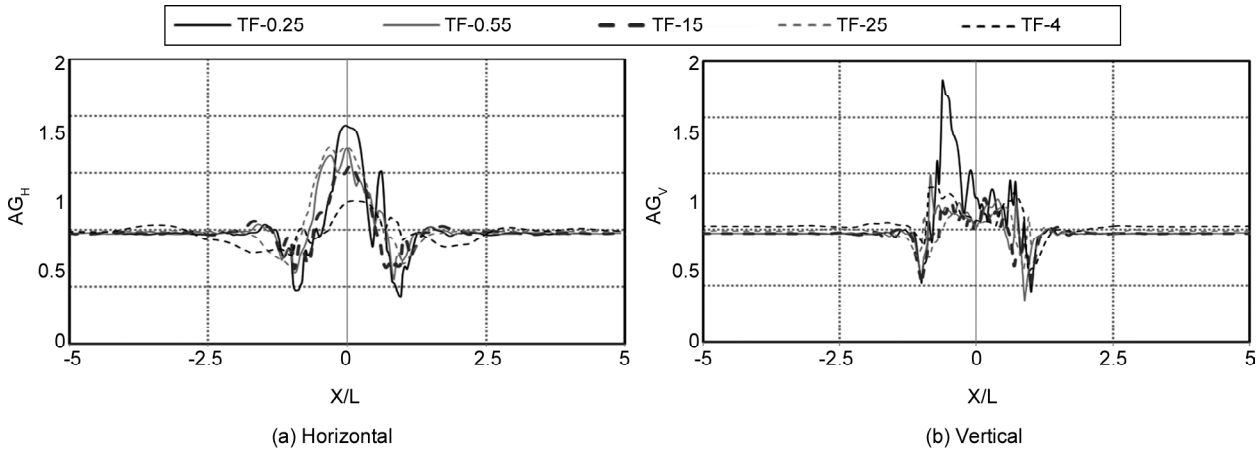

Figure 14. The variations of (a) horizontal and (b) vertical aggravation factors along the small trapezoidal basin models for different thickness factors.

assumed to be the same as those given in Table (2). A thickness factor (TF) is defined here as $H1$ to $H3$ ratio (Table 4). Figure (14) shows the variations of AG_H and AG_V factors for five assumed cases of thickness factor as listed in Table (4).

As the TF decreases, AG_H values increase in the center of the valley. In the case of TF-0.25, the AG_H of 1.5 appeared at $X / L = 0.6$, which show totally different behaviors from the other cases. The AGV shows almost the same trend with AG_H and its value increases with decreasing TF. It is noteworthy that the peak appearance of the AG_H and AG_V are opposite in $TF < 1$ and coincide in $TF > 1$.

Table 4. The variations of thickness parameters in the assumed models.

Thickness \ Case No.	TF-1/4	TF-1/2	TF-1	TF-2	TF-4
H (m)	210	150	120	150	210
H1 (m)	30	30	30	60	120
H2 (m)	120	60	30	30	30

7. Conclusions and Discussions

An attempt was made to comprehensively study 2D effects of small trapezoidal basin in regard with both excitation procedure and main features of small basin (slope angle, infill soil properties, basin length and thickness). Understanding of those effects could play an important role in design of critical facilities, lifelines, bridges, and so on. However, at irregular sites such as trapezoidal small basin, not only the soil properties, but also other important parameters could play an important role in site amplification and design motion characteristics. Furthermore, at laterally irregular site, the earthquake motions in different orthogonal directions are dependent and cannot be separately treated. These 2D features affect both the amplitude

and spatial variation of ground motions, which are the important parameters in design. The limited number of earthquake data recorded on small basins, and unknown subsurface geological conditions for some other data restrict the analysis of different small basins features to parametric study. Then, from extensive numerical analyses of small trapezoidal basin models, the following conclusions can be given:

1. A realistic result in numerical analysis of propagation media with lateral irregularity can be achieved by applying motions at least in two orthogonal directions.
2. The results from the frequency domain analysis, also show that not only the wave coupling occurs at the edges in two sides of trapezoidal basin, but also the interferences introduce new peak frequencies with different peak values, the appearance of which in the spectral ratios depend on the distance measuring point location with respect to basin edges.
3. For trapezoidal basin (basin with two slopes in both sides) the AG_H factors show value of 1.2 to 1.7 and AG_V factors show value of 1.5 to 2.3 in the middle of the basin. Furthermore, a very clear decrease in AG_H and AG_V values are seen in the basin slope locations.
4. The 2D effects of small basin are dominant in the distance range of $-2.5 < X / L > 2.5$ for trapezoidal small basins.
5. The maximum and minimum values of AG_H and AG_V factors relatively show large sensitivity to all basin assumed parameters variations.

From the above results, it is found that the response of the small basin is strongly 2D, and cannot possibly be captured by 1D soil response analysis. Finally, the above outcomes emphasize the need for including 2D analysis in design of the important facilities and infrastructures at the sites with a small basin, and provide an insight for including some rules or recommendations in design codes.

References

1. Takahashi, R. and Hirano, K. (1941) Seismic vibrations of soft ground. *Bull. Earthq. Res. Inst. Univ. Tokyo*, **19**, 534-543.
2. Aki, K. and Larner, K.L. (1970) Surface motion of layered medium having an irregular interface due to incident plane SH waves. *J. Geophys. Res.*, **75**, 933-954.
3. Kanai, K., Tanaka, T., and Yoshizawa, S. (1959) Comparative studies of earthquake motions on the ground and underground. *Bull. Earthq. Res. Inst. Univ. Tokyo*, **37**, 53-87.
4. Fishman, K.L. and Ahmad, S. (1995) Seismic response for alluvial valleys subjected to SH, P and SV waves. *Journal of Soil Dynamics and Earthquake Engineering*, **14**, 249-258.
5. Tumarkin, A.G. (1998) Site response analysis in 3D. *Proc. of the Int. Symp. on the Effects of Surface Geology on Seismic Motion*, Yokohama, Japan.
6. Paolucci, R. (1999) Numerical evaluation of the effect of cross-coupling of different components of ground motion in site response analyses. *Bull. Seismol. Soc. Am.*, **89**, 877-887.
7. Ghayamghamian, M.R. and Motosaka, M. (2003) The effects of torsion and motion coupling in site response estimation. *J. Earthq. Eng. Struct. Dyn.*, **32**, 691-709.
8. Ghayamghamian, M.R. (2008) Evidence for shear-wave coupling due to small-scale lateral irregularities, and the influence on site-response estimation. *Bull. Seismol. Soc. Am.*, **98**(3), 691-709.
9. Movahedasl, R. and Ghayamghamian, M.R. (2015) Effects of 2D small-scale sedimentary basins on strong ground motion characteristics. *Journal of Geophysics and Engineering*, **12**(4), 535-551.
10. Bard, P.Y., Campillo, M., Chavez-Garcia, F.J., and S?nchez-Sesma, F.J. (1988) The Mexico earthquake of September 19, 1985: A theoretical investigation of large and small amplification effects in the Mexico City Valley. *Earthquake Spectra*, **4**, 609-633.
11. Graves, R.W. (1996) Simulating realistic earthquake ground motions in regions of deep sedimentary basin. *Proc. of Eleventh World Conference on Earthquake Engineering*, Acapulco, Mexico, CD-ROM, No. 1932.

12. Kawase, H. and Matsushima, S. (1998) Strong motion simulation in Kobe during the Hyogoken Nanbu earthquake of 1995 based on a three dimensional basin structure. *J. Struct. Constr. Eng. Trans. Archit. Inst. Jpn.*, **514**, 111-118 (in Japanese).

13. Wald, D.J. and Graves, R.W. (1998) The seismic response of the Los Angeles basin. *Geophys. Res. Lett.*, 20, 403-406.

14. Sato, T., Graves, R.W., and Somerville, P.G. (1999) 3-D finite-difference simulations of long-period strong motions in the Tokyo metropolitan area during the 1990 Odawara earthquake (MJ 5.1) and the great 1923 Kanto earthquake (Ms 8.2) in Japan. *Bull. Seismol. Soc. Am.*, **89**, 579-607.

15. Semblat, J.F., Kham, M., Parara E, Bard, P.Y., Pitilakis, K., Makra, K., and Raptakis, D. (2005) Seismic wave amplification: basin geometry vs. soil layering. *Journal of Soil Dynamics and Earthquake Engineering*, **25**, 529-538.

16. Itasca, FLAC Version 7.00 (2012) A computer program for seismic response analysis for soil deposits. Itasca Consulting Group, Inc., Minneapolis, Minnesota, USA.

17. Lysmer, J. and Kuhlemeyer, R.L. (1969) Finite dynamic model for infinite media. *J. Eng. Mech.*, **95**(EM4), 859-877.

18. Rayleigh, J.W.S. and Lindsay, R.B. (1945) *The Theory of Sound*. Dover Publication, New York.

19. Kwok, A.O.L., Stewart, J.P., Hashash, Y.M.A., Matasovic, N., Pyke, R., Wang, Z., and Yang, Z. (2007) Use of exact solutions of wave propagation problems to guide implementation of nonlinear, time-domain ground response analysis routines. *ASCE Journal of Geotechnical and Geoenvironmental Engineering*, **133**(11), 1337-481.

20. Psarropoulos, P.N., Tazoh, T., Gazetas, G., and Apostolou, M. (2007) Linear and nonlinear valley amplification effects on seismic ground motion. *Soils and Foundation*, **47**(5), 857-871.

21. Ghayamghamian, M.R. and Kawakami, H. (1996) On the characteristics of non-linear soil response and dynamic soil properties using vertical array data in Japan. *Earthquake Engineering and Structural Dynamics*, **25**, 857-870.

22. Vucetic, M. and Dobry, R. (1991) effects of soil plasticity on cyclic response. *Journal of Geotechnical Engineering*, ASCE, 117, 89-107.

23. Tazoh, T., Dewa, K., Shimizu, K., and Shimada, M. (1984) Observations of earthquake response behaviour of foundation piles for road bridge. *Proc. 8th World Conference on Earthquake Engineering*, **3**, 577-584.

24. Tazoh, T., Shimizu, K., and Wakahara (1988) Seismic observations and analysis of grouped piles. *Shimizu Technical Research Bulletin*, **7**, 17-32.

25. Database advisory committee and working subcommittee (1993) *Strong Motion Array Record Database Association for Earthquake Disaster Prevention*, Report No. 1.

26. Yang, J. and Sato, T. (2000) Interpretation of seismic vertical amplification observed at an array site. *Bulletin Seism. Soc. Ame.*, **90**(2), 275-285.

27. Yang, J. and Yan, X. (2008) Site response to vertical earthquake motion. *Geotechnical Earthquake Engineering and Soil Dynamics*, **IV**, 1-8.